LAWRENCE
LIVERMORE
NATIONAL
LABORATORY

LLNL-JRNL-441091

Endomicroscopy imaging of epithelial structure using tissue autofluorescence

B. Lin, S. Urayama, R. M. G. Saroufeem, D. L. Matthews, S. G. Demos

July 9, 2010

Journal of Biomedical Optics

Disclaimer

Endomicroscopy imaging of epithelial structure using tissue autofluorescence

Bevin Lin[1,2], Shiro Urayama[3], Ramez M. G. Saroufeem[4],

Dennis L. Matthews[1,2], Stavros G. Demos[1,5]

[1]University of California, Davis NSF Center for Biophotonics Science & Technology, 4800 2nd Avenue, Sacramento, CA 95817

[2]University of California, Davis Department of Biomedical Engineering, One Shields Avenue, Davis, CA 95616

[3]University of California, Davis Medical Center, Division of Gastroenterology and Hepatology, 4150 V Street, Suite 3500, Sacramento, CA 95817

[4]University of California, Davis Medical Center, Department of Pathology, 4400 V Street, Sacramento, CA 95817

[5]Lawrence Livermore National Laboratory,7000 East Avenue, Livermore, CA 94550

ABSTRACT:

We explore autofluorescence endomicroscopy as a potential tool for real-time visualization of epithelial tissue microstructure and organization in a clinical setting. The design parameters are explored using two experimental systems – an Olympus Medical Systems Corp. stand-alone clinical prototype probe and a custom built bench-top rigid fiber conduit prototype. Both systems entail ultraviolet excitation at 266 nm and/or 325 nm using compact laser sources. Preliminary results using *ex vivo* animal and human tissue specimens suggest that this technology can be translated towards *in vivo* application to address the need for real-time histology and determine the basic design parameters for such instrumentation.

INTRODUCTION:

Late stage cancers visible at the tissue level are very difficult to treat. The current gold standard for histopathological diagnosis involves removal of tissue and lengthy preparation of biopsy specimens [1]. This prevents the availability of diagnostic information during the endoscopic procedure when it is most vital for patient care. It is believed that a critical component to future medical imaging would include techniques that provide non-invasive diagnosis of early stage disease and imaging of abnormal cellular development *in vivo*. A number of novel endomicroscopy techniques that provide real-time imaging of tissue microstructures have emerged in recent years accompanied by methods to generate contrast between sub-cellular components. Magnification chromoendoscopy includes topical application of contrast agents such as indigo carmine or acetic acid and has shown to be feasible and safe although several limitations have prevented widespread use [2]. Optical coherence tomography (OCT) provides images of major structural components of the mucosa and submucosa, at higher resolution than catheter probe endoscopic ultrasound [3] allowing visibility of normal squamous mucosa and specialized intestinal metaplasia in the esophagus, but has not yet been shown to adequately differentiate between dysplastic and intramucosal carcinoma [4]. Confocal fluorescence endomicroscopy uses spatial filtering to achieve cellular level imaging following intravenous administration of a fluorescing contrast agent, generally fluorescein, and is either integrated into distal tip of conventional upper endoscope, or as a dedicated stand-alone confocal miniprobe inserted through the accessory channel of a traditional endoscope [5-6]. Clinical teams tested the FDA-approved confocal endomicroscopy systems by Pentax Corporation [7-9] and Mauna Kea Technologies [10-

11]. While *in vivo* cellular imaging was successfully achieved, the image quality depends on fluorescein concentration and uptake, leakage, pattern distortion, and other complications directly related to intravenous fluorescein, including rare but serious adverse events [12]. Olympus Medical Systems Corp. has developed a magnification high-resolution endoscopy system [13-14] that has been shown to provide an increase in lesion detection of mucosal and vascular patterns by implementing white light (WL) and narrowband imaging (NBI), but did not provide imaging at the cellular level. Other white light (WL) endoscopic investigations include the use of contrast agents such as acriflavine hydrochloride [15], as well as quantum dots and gold nanoparticles [16].

Acquisition of diagnostic images without the use of contrast agents would arguably reduce cost and improve time efficiency in the operating room. Reflectance confocal endomicroscopy achieves a high degree of functionality [17-20], but typically requires a tissue preparation step to enhance visualization of the cell nuclei. Nonlinear techniques (such as two photon autofluorescence microscopy) use native tissue contrast mechanism [21-23] but implementation in a clinical environment would require the accommodation of complex instrumentation.

Imaging cellular level tissue structures using intrinsic contrast mechanisms, such as autofluorescence, requires the optimization of multiple parameters that govern image formation. These include optimization of the signal generation and collection efficiency and the mechanisms that provide contrast between sub-cellular components. To investigate this parameter space, this research team has explored a prototype

experimental Multimodal Microscope System (MMS) [24] to determine the most effective excitation-emission combinations [25]. We have recently demonstrated that wavelengths shorter than 355 nm penetrate only the superficial layer of cells resulting in acquisition of high contrast AF images of the epithelial layer using wide field microscopy [26]. It was also found that 266 nm excitation resulted in the best image contrast arising mainly from tryptophan emission and its non-uniform distribution within the cells [27]. These images of the epithelial layer may provide diagnostic information related to the presence and progress of disease. We hypothesize that since imaging can be achieved without the use of a signal intensive optical sectioning method (such as confocal on nonlinear excitation), the implementation of high signal throughput image acquisition designs could enable autofluorescence microscopic imaging of unprocessed tissue (no contrast agents or tissue preparation) at clinically relevant image acquisition times. In addition, adaptation of this non-contact imaging approach that provides cellular level resolution imaging without contrast agents into an endoscope probe for real-time *in vivo* imaging could provide a powerful tool for early detection of disease.

The objective of this research is to explore the possibility of implementing AF endomicroscopy for real-time *in vivo* visualization of epithelial tissue microstructure and organization in a clinical setting. The experimental approach is two-fold. We first adapted a clinical endosmicroscopy system developed by Olympus Medical Systems Corp. for wide-field endomicroscopy using narrow band imaging [28] to explore AF imaging under UV excitation. After evaluation of this system, we developed a bench-top endomicroscopy prototype (BEP) that incorporates solutions to issues identified using the

Olympus system. The results suggest that AF endomicroscopy could forge a path towards providing *in vivo* histopathology information to help determine the basic design parameters for such clinical instrumentation.

Animal and Human tissue preparation

Murine kidney was chosen as the animal model due to the well-defined structure in the microscopic level where cells on the order of 10 μm in diameter form tubules with diameters of 50 μm to 80 μm. Kidney specimens were obtained from animals that were euthanized under general anesthesia approved by the University of California, Davis, Animal Use and Care Administrative Advisory Committee.

Human biopsy specimens from patients undergoing routine surveillance for Barrett's esophagus were collected in accordance with a protocol approved by the Institutional Review Board (IRB) at the University of California, Davis Medical Center. Standard forceps were used during endoscopy to collect one biopsy specimen from the vicinity of the squamocolumnar junction (Z-line), one from the gastroesophageal (GE) junction, and one from the proximal stomach (cardia) for a total of three biopsy specimens per patient. Each specimen was immediately placed in an individually labeled container with Roswell Park Memorial Institute (RPMI) 1640 media (Invitrogen, Carlsbad, CA) and transported to the imaging lab located in the same building where the AF microscopy measurements were taken. Immediately after completion of the imaging experiments, each tissue biopsy specimen was individually placed in 10% formalin jar for fixation and transferred to pathology for tissue diagnosis. The pathological evaluation was confirmed by at least

two expert pathologists and taken as the diagnostic gold standard from which the optical images were categorized.

Experiments and Results Using Olympus Endo-Cytoscopy System

A clinical prototype developed by Olympus Medical Systems Corp., Tokyo, Japan designed to provide contrast enhanced fluorescence imaging using methylene blue [29] and/or narrow-band illumination [30] was used to test the AF microscopic imaging approach under UV excitation. This Endo-Cytoscopy System (ECS) was designed to be used in contact mode and has not been used for AF measurements before. This system is also not compatible with transmission of UV excitation. It provides image acquisition of a 350 μm x 350 μm field of view at a frame rate of 30 Hz. For the purpose of integrating AF imaging under UV laser excitation into this system without altering existing hardware, a simple image relay approach was adapted to enable the off-axis UV laser excitation beam to reach the tissue and maintain reasonably high signal collection efficiency. A schematic of this image relay design is depicted in Fig. 1(a). Using white light and a positive back-*illuminated* USAF 1951 resolution target (Edmund Optics Inc., Barrington, NJ), the spatial resolution of the ECS after relay was estimated to be on the order of 3 to 4 μm as shown in the inset of Fig 1(b).

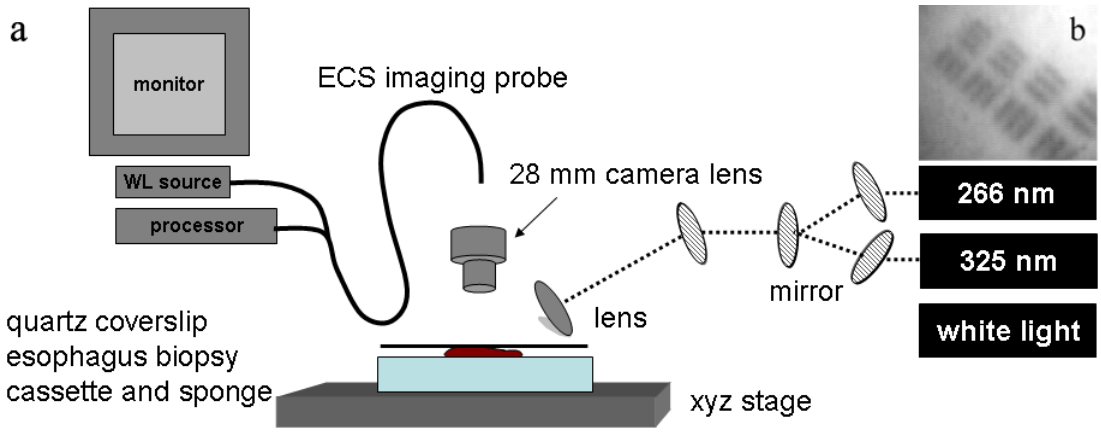

Fig. 1: Schematic diagram (a) of image relay design to adapt AF microscopy under 266 nm and 325 nm excitation into the ECS prototype. Inset (b) shows the image of the resolution target with size of smaller lines at 2.2 µm..

The ECS probe was secured to a stage mobile in the xyz directions and located directly above a 28 mm camera lens to collect AF emission in the visible spectral range and image relay to the imaging plane of the ECS probe. This standard Nikon lens was chosen to preserve the 1:1 imaging ratio, provide a working distance of about 3 cm and provide high signal collection efficiency. The unprocessed tissue specimen was placed under a quartz cover slip and centered on a sponge in a standard pathology cassette to maintain tissue moisture during imaging. The cassette was positioned on a second xyz stage directly below the Nikon lens.

The excitation laser sources used to excite the tissue specimens in order to acquire the AF images with the ECS were a 266 nm laser (Intelite, Inc., Minden, NV) and a 325 nm laser (Omnichrome, Melles Griot, Carlsbad, CA). A converging lens was used to concentrate the excitation laser beam onto the tissue sample to an area of about 3 mm^2 centered at the

location of the tissue that is imaged by the ECS. The UV exposure to the tissue surface was about 0.5 mW for the 266 nm excitation and 4 mW for 325 nm excitation. Experiments performed using the MMS platform that have been reported elsewhere have suggested that emission from tryptophan predominates the autofluorescence signal under 266 nm excitation, while NADH and collagen emission are the main contributors under 355 nm excitation [27].

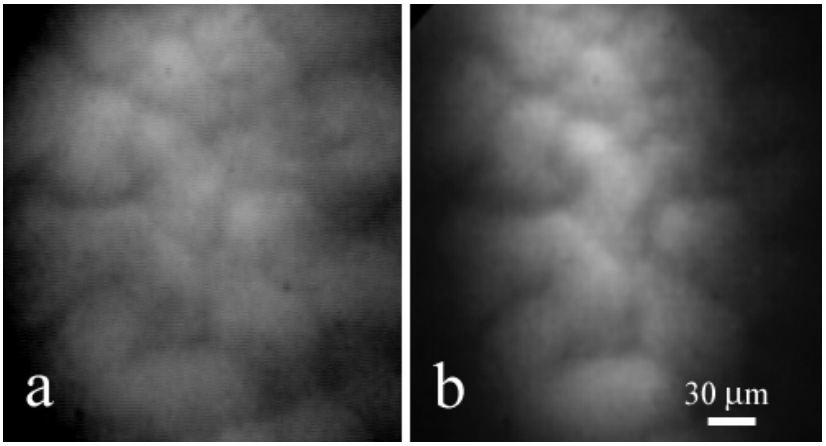

Fig. 2: AF image of a same region of a murine kidney specimen with the capsule removed under a) 325 nm, and b) 266 nm excitation.

Fig. 2 shows AF microscopic images of the same location from an unprocessed murine kidney under 266 nm and 325 nm excitation in the 410 nm – 800 nm spectral range (determined by the spectral response of the ECS probe). The images were acquired without any preparation to the sample. The outlines of the tubule structures are visible under both excitation wavelengths. The image shown in Fig. 2a is similar (considering the lower spatial resolution) to those obtained under 355 nm excitation using the MMS platform. However, although it was expected that the nuclei would be visible under 266 nm excitation (as shown in previous studies [25]), the image in Fig. 2(b) did not provide

the expected nuclei visibility or contrast. It must be noted that the low exposure of the camera of the ECS probe (at 30 Hz frame rate) required increased photo-excitation to provide sufficient AF signal to be recorded by the camera. As tryptophan is the main fluorophore contributing to the image formation and contrast under 266 nm excitation, we hypothesized that photobleaching of tryptophan may be responsible for the loss of visualization of the nuclei. To test this hypothesis, we used the MMS platform to monitor the visualization and contrast of murine kidney cell nuclei as a function of power of the 266 nm excitation. We found that increased exposure to 266 nm light leads to loss of nuclei visibility and an overall reduction in signal intensity. These results identified a limitation of this approach that can be mitigated by reducing the exposure to 266 nm excitation which in turn would require image acquisition at a lower (than 30 Hz) frame rate.

Understanding these limitations, we used the ECS probe for imaging experiments of human tissue specimens obtained from eight patients. Human esophageal tissue was imaged with the same approach as the animal tissue, using both 325 nm and 266 nm laser excitation. The experimental results are exemplified in Fig. 3.

Large round structures are obvious in the esophagus tissue image shown in Fig. 3(a). These rosette features are typical of gastric mucosa and can be expected, as the esophagus biopsy specimen was collected from columnar epithelial region within Barrett's esophagus. This was consistent with preliminary results using the MMS platform [31]. The biopsy specimen collected at the squamocolumnar junction (Z-line)

clearly displays the characteristic honeycomb pattern of columnar mucosa, visible in Fig. 3(b). These AF results correlate with the gold standard H&E inset and with previous imaging experiments under 266 nm excitation using the MMS platform [26]. The need for increased AF signal and contrast as well as reduced exposure to avoid photobleaching of tryptophan made the image relay system design difficult at the manufacturer-fixed 30 Hz frame rate. Reducing the 266 nm laser power resulted in insufficient AF signal and loss of image acquisition. It is evident that a digital camera that would allow for longer exposure times would have offered a solution to this problem.

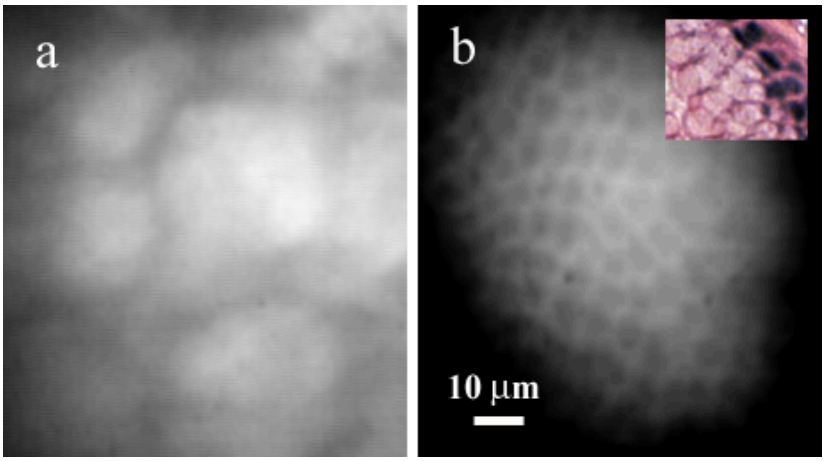

Fig. 3: AF images of *ex vivo* human esophagus specimens using a clinical endomicroscopy prototype system developed by Olympus under a) 325 nm excitation with resulting AF image of gastric-type mucosa, and b) 266 nm excitation with resulting AF image of columnar mucosa. Gold standard 57 μm x 48 μm H&E inset of typical honeycomb pattern of columnar mucosa.

Experiments and Results Using the Bench top Endomicroscopy Prototype (BEP)

With the experience attained using the ECS probe, we have developed a bench-top prototype that addresses some of the limitation but preserves the overall concept for

translation to a future endomicroscope system. The operational parameters of this prototype system were explored using animal and human tissues. Fig. 4 shows a schematic diagram of this bench-top endomicroscope prototype (BEP). The system was secured in a vertical position above a sample holder. To maintain moisture in the tissue during imaging, the specimens were covered with a quartz cover slip and placed in a standard pathology cassette and sponge. The cassette was positioned directly below a 0.4 numerical aperture ×20 quartz objective that transmits 266 nm excitation (Thorlabs, Newton, New Jersey) and provides a 4 mm working distance. A compact diode-pumped solid state laser operating at 266 nm (Intelite, Inc., Minden, NV) was coupled to a UV compatible fiber. The fiber output was first collimated using a converging lens and then, using a second lens, it was refocused in front of the microscope objective lens after it was coupled into the microscope's imaging path using a UV dichroic mirror. The combination of the two lenses and the microscope objective provide for magnification and imaging of the output of the excitation fiber to an area of about 3 μm^2 centered within the imaged area of the specimen. The AF signal collected by the microscope objective was used to form an image of the illuminated area of the specimen in the input plane of an imaging fiber conduit (Edmund Optics Inc., Barrington, NJ). The fiber conduit was 6 inches in length with an outer diameter of 3.2 mm. The diameter of each individual fiber was 12 μm resulting in a fiber count of 50,419. These fibers were the effective image pixels when the image was transported through the fiber conduit. This image preserving fiber conduit was not UV compatible and as a result, only the AF signal in the visible range was transmitted to the output side of the conduit. The image at the output side was then projected using an achromat lens (OFR/Thorlabs, Caldwell, NJ) onto a thermoelectrically

cooled detector (Photometrics, Tucson, AZ). In this arrangement, each individual fiber of the conduit was projected on about 6x6 pixels in the CCD detector. The CCD, lens system, objective, and tissue stage were each mounted on xyz stages that enabled rapid alignment and focusing of individual components. The spatial resolution of the BEP system was better than 2.2 μm as it was determined using white light and a back-illuminated positive USAF 1951 resolution target (see inset in Fig 4). For imaging of the specimens, the detector's pixels were binned (4x4 pixel binning) without loss of image resolution as this was determined by the projected size of the individual fibers of the conduit (6x6 pixels). Using a laser power of about 500 μW at the sample location (for an approximate dose of 8 mJ/cm^2), the images were acquired under 0.5 second exposure yielded images with a digitized intensity of about 3000 counts per pixel.

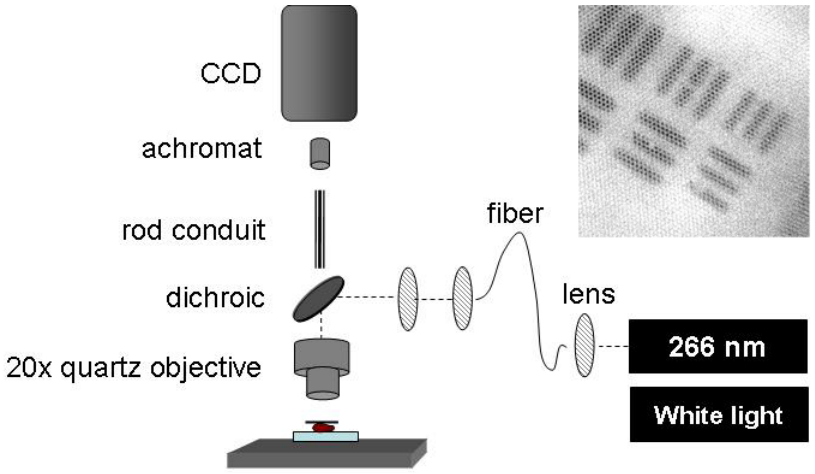

Fig. 4: Schematic diagram of rod conduit image relay design of the bench-top prototype system. Inset shows the image of the resolution target with size of smaller lines at 2.2 μm.

An individual tubule from a fresh rat kidney specimen is clearly defined and easily recognized in Fig. 5 under 266 nm excitation. The darker features within the tubules are

believed to be the cell nuclei as indicated with comparison to the H&E cross-section inset and previous studies using the MMS platform [24].

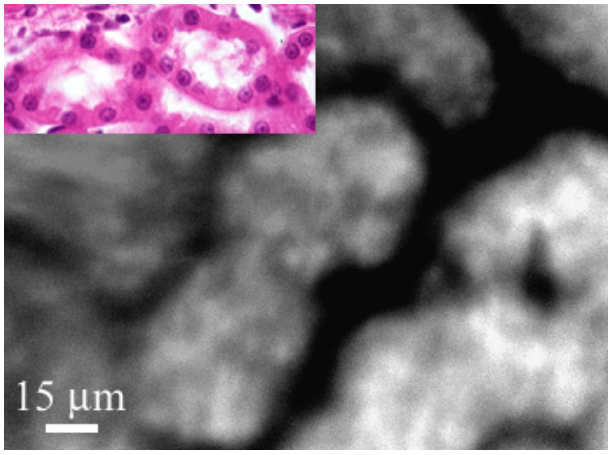

Fig. 5: AF image of fresh rat kidney specimen (225 µm x 168 µm) under 266 nm excitation.

Specimens from a total of 6 patients were imaged with this bench top prototype. Human stomach specimens were imaged with the same approach as the animal tissue using 266 nm laser excitation. Representative round cluster of gastric cells exemplified in the H&E stained specimen of Fig. 6(a) correspond to the visible AF imaged structures in Fig. 6(b), and are also similar to the gastric-type esophageal cells of Fig. 3(a).

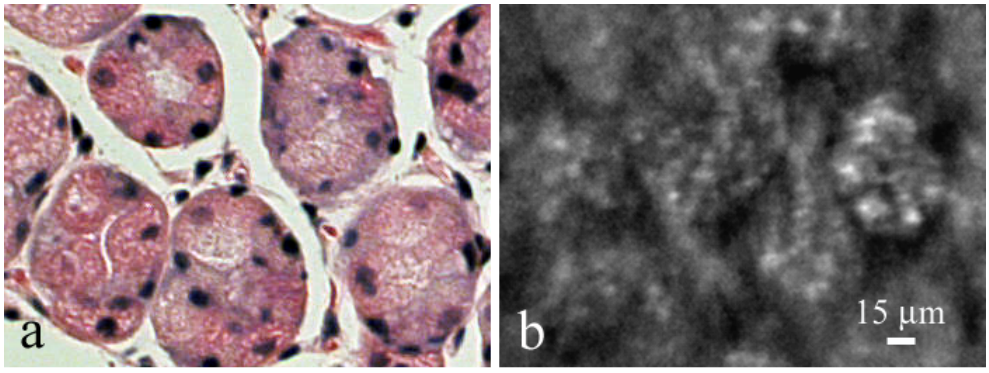

Fig. 6: 225 µm x 168 µm field of view of human stomach epithelium biopsy specimen of a) surface sliced H&E and b) fiber conduit under 266 nm exposure. Rosette-like features can be appreciated in both images.

DISCUSSION

The experimental results demonstrate a proof of principle transition to wide-field endomicroscopy using tissue autofluorescence under UV excitation. The results obtained using the ECS prototype provided cellular resolution of murine kidney tubules (Fig. 2) and human esophageal gastric-type and glandular mucosa (Fig. 3) without contrast agents. Higher quality images were obtained using the BEP system.

The AF images obtained using the BEP system were acquired under an approximate dose of 8 mJ/cm^2, slightly above the ANSI defined maximum permissible exposure (MPE) for exposure to UV wavelengths between 180 nm – 302 nm of 3 mJ/cm^2 [32]. There are multiple improvements in the system's components that can reduce the required dosage by more than one order of magnitude. Most important is the appropriate selection of the image transporting optical element which in our case was the image preserving fiber conduit. This fiber conduit is only transmitting the emission at wavelengths longer than

about 400 nm. Therefore, as the autofluorescence signal under 266 nm excitation is mostly due to tryptophan, only a small portion of this signal (on the order of 10%) was transmitted through the image transporting fiber conduit. Using a UV compatible image transporting element would increase the signal available to be detected by the CCD detector by about one order of magnitude. Furthermore, the CCD detector used for image acquisition has only about 30% QE between 400 nm – 450 nm (which covers the spectral range where most of the detected signal is located). Therefore, appropriate selection of the CCD detector to provided optimized sensitivity in the 300-500 nm spectral range can enhance signal detection efficiency by another factor of about 2X. Finally, the recorded image had a pixel intensity of about 3000 counts. There is no need to record images with this high pixel intensity since images with 1/5 of this intensity cannot be distinguished by the observer in a clinical setting based on image quality (signal noise and image contrast) from those recorded during our experiments. Hence, only these three improvement discussed above can lead to reduction in the required exposure dose by about 100X compared to the dose of about 8 mJ/cm^2 used during our experiments.

The small 225 μm x 168 μm field of view (FOV) of the BEP system is due to the limited number of fibers of the image transport conduit. In order to achieve spatial resolution on the order of 1 μm, the magnification in the front end of the system was adjusted so that an area of about 1 μm^2 at the tissue plane is projected into a single fiber at the input of the fiber conduit. It can be appreciated that using a different image transport system it is possible to increase the FOV without loss of spatial resolution. For example, using an image transport system that preserves the spatial resolution at the input plane (such as a

rod lens system), the FOV can be increased to more than 1 mm^2 (determined by the pixel size and number of the CCD camera). This in turn would greatly enhance the ability to screen larger tissue areas within clinical relevant times compared to confocal systems.

The elimination of contrast agents will arguably improve safety, cost, and time efficiency. Current surveillance guidelines during upper endoscopy procedures collect random four quadrant biopsies every one to two centimeters throughout the length of columnar epithelium in the Barrett's esophagus. The pathology cost to Medicare alone for a single jar of four biopsies is substantial. Thus, a technology that could reliably identify cellular level changes indicative of premalignancy has the potential to dramatically reduce the need and cost of random biopsies [6, 33]. Integration of an endomicroscopy technique such as the method discussed in this work with conventional endoscopy to determine regions of interest for directed biopsy may be the most efficient approach in terms of technical feasibility and integration of information provided by novel technology with current state-of-the-art clinical practice. Optical capabilities and parameters of our current bench top prototype (BEP) can be easily implemented into endoscopic embodiments to provide real-time *in vivo* diagnostic information.

This UV AF imaging methodology using excitation wavelengths that cover the spectral range for tryptophan absorption clearly provides the contrast and spatial resolution necessary to distinguish normal and abnormal esophageal structures at the cellular level based on morphological change. Experimental results presented elsewhere [27] suggest that the mechanism behind the imaging of the superficial tissue layer using wide field

microscopy designs is due to the UV excitation light only penetrating tissue to about 100 μm or less, the approximate thickness of the image plane. As a result, a sufficient amount of the fluorescence signal produced in the superficial tissue layer can be contained within the thickness of the image plane of the microscope, thus the out-of-focus signal is sufficiently reduced to allow the formation of high contrast images without the need to use spatial filtering. We are currently working on the development of guidelines for interpreting the AF images obtained from a wide variety of pathological conditions to provide rules of interpretation for enabling *in vivo* histopathologic evaluation.

A future system would ideally include both the macro and micro imaging capabilities to first survey a large surface area with smooth transition for detection from tissue to cell level via a zoom lens. Mapping capabilities would enable more direct correlation between optical and histopathological recognition. Additionally, the sensitivity and specificity for premalignant conditions such as dysplasia must be substantiated. Deformable liquid optics may be a key part of such future designs.

Pulsed illumination may be another method of optimizing AF imaging while better controlling the delivery of the laser energy to the tissue. Taking into account that the emission lifetime of the tissue chromophores is on the order of 10 nsec, the overall time-frame needed for image acquisition could be approximately 20 nsec. Using pulsed excitation can be an effective solution to this problem as it enables image acquisition much faster than the tissue can move beyond the instrument's specified spatial resolution

of, and relative to, the imaging system. An uncooled CCD (or other type of array detector) could capture this signal without thermal noise problems typically associated with prolonged acquisition times. This is also important for the miniaturization of the instrument such as placing the CCD detector at the tip of an endoscope. *In vivo* imaging can be plagued with motion artifacts due to intrinsic micro- and macro- vasculature and musculature movements such as circulation and breathing that could ultimately limit *in vivo* application [34]. Thus, the image quality of an *in vivo* microscope system depends not only on the design characteristics of the optical components but also the degree to which the object being imaged can be kept immobilized with respect to the imaging system during image acquisition.

Acknowledgements

We thank Dr.s Kazuhiro Gono, Takeshi Ozawa, and Nobuyuki Doguchi of Olympus Medical Systems Corp. for lending us the Endo-Cytoscopy System. We also thank Chris Pivetti for supplying murine kidney specimens. This work performed in part under the auspices of the U.S. Department of Energy by Lawrence Livermore National Laboratory under Contract DE-AC52-07NA27344. This research is supported by funding from the Center for Biophotonics, an NSF Science and Technology Center, managed by the University of California, Davis, under Cooperative Agreement No. PHY 0120999.

References

1. B. Young, Heath, J.W., *Wheater's Functional Histology* (Elsevier Limited, 2000).

2. R. Davila, "Chromoendoscopy," Gastroenterol. Clin. North Am. **19**, 193-208 (2009).

3. A. Das, M. V. Sivak, A. Chak, R. C. K. Wong, V. Westphal, A. M. Rollins, J. Willis, G. Isenberg, and J. A. Izatt, "High-resolution endoscopic imaging of the GI tract: a comparative study of optical coherence tomography versus high-frequency catheter probe EUS," Gastrointest. Endosc. **54**, 219-224 (2001).

4. J. A. Evans, J. M. Poneros, B. E. Bouma, J. Bressner, E. F. Halpern, M. Shishkov, G. Y. Lauwers, M. Mino-Kenudson, N. S. Nishioka, and G. J. Tearney, "Optical coherence tomography to identify intramucosal carcinoma and high-grade dysplasia in Barrett's esophagus," Clin. Gastroenterol. Hepatol. **4**, 38-43 (2006).

5. S. Kantsevoy, D. Adler, J. Conway, D. Diehl, F. Farraye, V. Kaul, S. Kethu, R. Kwon, P. Mamula, and S. Rodriguez, "Confocal laser endomicroscopy," Gastrointest. Endosc. **70**, 197-200 (2009).

6. M. Wallace, and P. Fockens, "Probe-Based Confocal Laser Endomicroscopy," Gastroenterology **136**, 1509-1513 (2009).

7. K. Dunbar, P. Okolo, E. Montgomery, and M. Canto, "Confocal laser endomicroscopy in Barrett's esophagus and endoscopically inapparent Barrett's neoplasia: a prospective, randomized, double-blind, controlled, crossover trial," Gastrointest. Endosc. (2009).

8. C. Gheorghe, R. Iacob, G. Becheanu, and M. Dumbrava, "Confocal endomicroscopy for in vivo microscopic analysis of upper gastrointestinal tract premalignant and malignant lesions," J. Gastrointestin. Liver Dis. **17**, 95-100 (2008).

9. M. Wallace, "Leeuwenhoek Meets Kussmaul: The Evolution of Endoscopist to Endo-Pathologist," Gastroenterology **131**, 347-349 (2006).

10. A. Meining, "Confocal Endomicroscopy," Gastrointest. Endosc. Clin. N. Am. **19**, 629-635 (2009).

11. T. D. Wang, S. Friedland, P. Sahbaie, R. Soetikno, P. L. Hsiung, J. T. C. Liu, J. M. Crawford, and C. H. Contag, "Functional imaging of colonic mucosa with a fibered Confocal microscope for real-time in vivo pathology," Clin. Gastroenterol. Hepatol. **5**, 1300-1305 (2007).

12. M. Wallace, A. Meining, S. Miehlke, T. Rosch, H. Pohl, C. Lightdale, B. Filoche, D. Carr-Locke, E. Coron, and J. Moreau, "Safety of Intravenous Fluorescein for Probe-Based Confocal Laser Endomicroscopy (pCLE): A Multicenter Study," Gastrointest. Endosc. **69** (2009).

13. G. K. Anagnostopoulos, K. Yao, P. Kaye, C. J. Hawkey, and K. Ragunath, "Novel endoscopic observation in Barrett's oesophagus using high resolution magnification endoscopy and narrow band imaging," Aliment. Pharmacol. Ther. **26**, 501-507 (2007).

14. W. L. Curvers, R. Singh, L. M. W. K. Song, H. C. Wolfsen, K. Ragunath, K. Wang, M. B. Wallace, P. Fockens, and J. J. G. H. M. Bergman, "Endoscopic tri-modal imaging for detection of early neoplasia in Barrett's oesophagus: a multi-centre feasibility study using high-resolution endoscopy, autofluorescence imaging and narrow band imaging incorporated in one endoscopy system," Gut **57**, 167-172 (2008).

15. T. Muldoon, S. Anandasabapathy, D. Maru, and R. Richards-Kortum, "High-resolution imaging in Barrett's esophagus: a novel, low-cost endoscopic microscope," Gastrointest. Endosc. **68**, 737-744 (2008).

16. J. Rogers, S. Landau, T. Tkaczyk, M. Descour, M. Rahman, R. Richards-Kortum, A. Kärkäinen, and T. Christenson, "Imaging performance of a miniature integrated microendoscope," J. Biomed. Opt. **13**, 054020 (2008).

17. L. Gao, R. Kester, and T. Tkaczyk, "Compact Image Slicing Spectrometer (ISS) for hyperspectral fluorescence microscopy," Opt. Express **17**, 12293-12308 (2009).

18. R. Kester, T. Tkaczyk, M. Descour, T. Christenson, and R. Richards-Kortum, "High numerical aperture microendoscope objective for a fiber confocal reflectance microscope," Opt. Express **15**, 2409-2420 (2007).

19. M. Nakao, S. Yoshida, S. Tanaka, Y. Takemura, S. Oka, M. Yoshihara, and K. Chayama, "Optical biopsy of early gastroesophageal cancer by catheter-based reflectance-type laser-scanning confocal microscopy," J. Biomed. Opt. **13**, - (2008).

20. H. Shin, M. Pierce, D. Lee, H. Ra, O. Solgaard, and R. Richards-Kortum, "Fiber-optic confocal microscope using a MEMS scanner and miniature objective lens," Opt. Express **15**, 9113-9122 (2007).

21. C. Li, C. Pitsillides, J. M. Runnels, D. Coˆte´, and C. P. Lin, "Multiphoton Microscopy of Live Tissues with Ultraviolet Autofluorescence," IEEE J. Sel. Top. Quant. 10.1109/JSTQE.2009.2031619 (2009).

22. D. Li, W. Zheng, and J. Qu, "Imaging of epithelial tissue in vivo based on excitation of multiple endogenous nonlinear optical signals," Opt. Lett. **34**, 2853-2855 (2009).

23. W. Rice, D. Kaplan, and I. Georgakoudi, "Quantitative biomarkers of stem cell differentiation based on intrinsic two-photon excited fluorescence," J. Biomed. Opt. **12**, 060504 (2007).

24. S. G. Demos, C. A. Lieber, B. Lin, and R. Ramsamooj, "Imaging of tissue microstructures using a multimodal microscope design," IEEE J. Sel. Top. Quant. **11**, 752-758 (2005).

25. B. Lin, Lieber, C.A., Fitzgerald,J.T., Michalopoulou, A.P., Raman, R.N., Pivetti, C.D, Troppmann, C., Matthews, D.L., Demos, S.G., "Real-time Imaging of Tissue Microstructures Using Intrinsic Optical Signatures," in *SPIE Photonics West BiOS Optical Biopsy VI*, A. K. Robert R. Alfano, ed. (San Jose, CA, 2006).

26. B. Lin, S. Urayama, R. M. G. Saroufeem, D. L. Matthews, and S. G. Demos, "Real-Time Microscopic Imaging of Esophageal Epithelial Disease with Autofluorescence under Ultraviolet Excitation," Opt. Express **17** (2009).

27. B. Lin, S., Urayama, R.M.G., Saroufeem, D.L., Matthews, S.G., Demos, "Characterizing the origin of autofluorescence in human esophageal epithelium using ultraviolet spectroscopy and microscopy," Manuscript submitted for publication to "Optics Express".

28. K. Gono, "Multifunctional endoscopic imaging system for support of early cancer diagnosis," IEEE J. Sel. Top. Quant. **14**, 62-69 (2008).

29. Y. Kumagai, K. Monma, and K. Kawada, "Magnifying chromoendoscopy of the esophagus: in-vivo pathological diagnosis using an endocytoscopy system," Endoscopy **36**, 590-594 (2004).

30. K. Gono, T. Obi, M. Yamaguchi, N. Ohyama, H. Machida, Y. Sano, S. Yoshida, Y. Hamamoto, and T. Endo, "Appearance of enhanced tissue features in narrow-band endoscopic imaging," J. Biomed. Opt. **9**, 568 (2004).

31. B. Lin, S., Urayama, R.M.G., Saroufeem, D.L., Matthews, S.G., Demos, "Early identification and establishment of rules for interpretation of endoscopically invisible intestinal metaplasia using ultraviolet autofluorescence for real-time histology," Manuscript in Preparation.

32. T. L. I. o. America, "American National Standard for Safe Use of Lasers Z136.1," (2000).

33. J. Inadomi, R. Sampliner, J. Lagergren, D. Lieberman, A. Fendrick, and N. Vakil, "Screening and surveillance for Barrett esophagus in high-risk groups: a cost-utility analysis," Ann. Intern. Med. **138**, 176 (2003).

34. H. C. Wolfsen, "New Technologies for Imaging of Barrett's Esophagus," Surg. Oncol. Clin. N. Am. **18**, 487-502 (2009).